Surfactant-Assisted Electrodeposition of CoFe-Barium Hexaferrite Nanocomposite Thin Films

S. Kharratian Khameneh[1], M. Heydarzadeh Sohi[1], A. Ataie[1]

Abstract

The influences of anionic sodium dodecylsulfate (SDS) and cationic Hexadecyltrimethylammonium bromide (HTAB) surfactants on the incorporation and distribution of barium hexaferrite nanoparticles in the electrodeposited CoFe-$BaFe_{12}O_{19}$ composite thin films were studied. Sulphate bathes with natural pH containing 0 to 2 g/L surfactants were used for electroplating at room temperature. Field emission scanning electron microscopy (FE-SEM) and energy dispersive spectroscopy (EDS) from the surface of the deposited films, together with X-ray diffraction analysis were applied to confirm codeposition of the iron and cobalt, as well as incorporation of the nanoparticles. The results showed that the amounts of hexaferrite particles in the deposits were initially increased by increasing the concentrations of both surfactants in the electrolyte and reduced by further additions of the surfactants. The optimum values of surfactants were 1 and 0.5 g/L for SDS and HTAB, respectively. The highest amount of the barium hexaferrite in the deposits was 12 wt% which was achieved by using an electrolyte containing 0.5 g/L HTAB surfactant. Composition of the film's matrix was also changed by varying the amounts of the surfactants. The variation of the iron content of the film's matrix appeared to follow a trend similar to that of the amount of the particle's incorporation. The films deposited from electrolytes containing HTAB showed coarser morphologies compared to those obtained from bathes without surfactant or containing SDS.

Keywords: Nanocomposite thin films; Electrodeposition; CoFe alloy; Ultrasonic; Barium hexaferrite; Surfactants

1. Introduction

Recent studies show that electromagnetically-actuated micro/nano electromechanical systems (MEMS/NEMS) offer reversible effect, high speed actuation, long-distance transmission of an intense force, less susceptibility to malfunction in harsh environments (dust, humidity), and are actuated with low cost voltage controllers. Both hard and soft magnetic materials are applied in fabrication of magnetic MEMS/NEMS including microactuators, sensors, micromotors, frictionless microgears and recording heads [1-5]. Designing new materials like magnetic soft-hard composites which combine the hard magnetic properties such as high coercivity with the high saturation magnetization achievable in soft magnetic materials, seems to be a great progress in this field. On the other hand, application of magnetic thin films provide MEMS/NEMS devices with significant advantages such as reduction in size, high stored energy, high force, operation at room temperature, etc. When hard-magnetic particles are inserted into soft thin films, the interest is mainly focused on the possibility of producing functional permanent magnets at micro and nano scale for implementation in microactuators devices [6-10].

Among a diversity of fabrication techniques, electrochemical processes are very promising for deposition and integration of magnetic thin films into MEMS/NEMS, since they provide a good compromise in various aspects. Electrodeposition is well-suited to fulfill the requirements of high yield and cost effective processes [3, 9]. This method offers many advantages, including room temperature operation, low energy consumption, fast

1- School of Metallurgy and Materials Engineering, College of Engineering, University of Tehran, Tehran, Iran.

Corresponding author: M. Heydarzadeh Sohi, School of Metallurgy and Materials Engineering, College of Engineering, University of Tehran, Tehran, Iran.
Email: mhsohi@ut.ac.ir

deposition rates which lead to high thickness of films, fairly uniform deposition over complicated shapes, low cost, simple scale-up, and easily maintained equipment. Moreover, the properties of the deposits can be "tailored" by controlling solution compositions and deposition parameters. It is also possible to codeposit a variety of metallic elements together with inert particles that are insoluble in deposition bath [2,3,9-11].

Surfactants are usually used in electroplating solutions for codeposition of particles with metal matrix. Addition of a surfactant improves particles suspension in the electrolyte by increasing wettability and surface charge of the suspended particles, hence prevents agglomeration of the particles and facilitates deposition procedure. Anionic surfactants are particularly interesting because they can inhibit hydrogen evolution and subsequently pin pores in the electrodeposited films. Moreover, they can form complexes with metal ions, which suppress precipitation of adverse hydroxides during electrodeposition. However, since deposition takes place on the cathode, a cationic surfactant will favour the particle-cathode electrostatic attraction. Consequently it can promote the codeposition and increase uniformity of particles in the composite layers. Anionic surfactant SDS (sodium dodecylsulfate $CH_3(CH_2)_{11}SO_4Na$) and cationic surfactant HTAB (hexadecyltrimethylammonium bromide $CH_3(CH_2)_{15}(CH_3)_3NBr$) are frequently used in electrodeposition [12-16].

The present work aims to prepare CoFe-barium hexaferrite nanocomposites using the aforementioned surfactants, to assure entrapment of a large amount of particles in the deposited films. Cobalt–iron alloys have been chosen because they show the highest saturation induction (2.45 T for the 35% Co alloy) among ferromagnetic materials at room temperature. As a result, these alloys can be considered as a very good choice in magnetic MEMS/NEMS. These materials also have large magnetocrystalline anisotropy and magnetostriction [17-20]. Barium hexaferrite has significant potential for being used as permanent magnets and microwave absorbing coatings, because of its adequate combination of high Curie temperature, high coercivity and chemical stability [21,22].

2. Experimental

An optimized electroplating bath containing 0.08 mol dm^{-3} $CoSO_4.7H_2O$ + 0.015 mol dm^{-3} $FeSO_4.7H_2O$ + 25 g dm^{-3} boric acid + 20 g dm^{-3} sodium citrate + 20 g dm^{-3} barium hexaferrite containing 0 to 2 g dm^{-3} SDS and CTAB was chosen. Barium hexaferrite nanoparticles were synthesized through a co-precipitation route and had plate-like morphology with mean diameter of 300 nm and thickness of 45 nm [23]. All reagents were of analytical grade and solutions were freshly prepared with distilled water.

Pulsed current was used for electrodeposition at room temperature and the pH of the electrolyte was natural (~5). Platinum foil was used as non-consumable anode and brass sheets (as non-magnetic materials) were employed (Area=2 cm^2) as cathode. The substrate was first cleaned with alcohol followed by immersing in 5 vol% HCl solution to remove organic impurities and the natural oxide layer on the surface. A current density of 15 mA/cm^2 was applied and the plating time was 30 minutes. Deposition was performed after keeping particles in suspension for 30 min, using a rod stirrer at moderate stirring rate (900 rpm). The electrolytic bath was also mechanically stirred at a lower rate (500 rpm), during the electroplating.

Finally, the electroplated samples were subjected to ultrasonic cleaning process in the ethanol to remove the surplus barium hexaferrite nanoparticles.

The phase identification of the specimens was performed using a Philips X' Pert Pro X-ray diffraction (XRD) system. A Cu-Kα radiation operating at 30 kV and 20 mA and 2θ range between10 to 80° with a step range of 0.02° and a measuring time of 0.35 s per step was used for difractometry.

Surface morphologies of deposits were observed using a Hitachi Su8040 field emission scanning electron microscope (FE-

SEM) and the compositions of deposits were determined by energy-dispersive X-ray spectroscopy (EDS).

3. Result and Discussion

Elemental analysis of the films deposited in absence or presence of the surfactants confirmed incorporation of barium hexaferrite particles to the films. Fig. 1 shows the EDS spectrum for the CoFe-$BaFe_{12}O_{19}$ composite film deposited from a surfactant-free bath containing 20 g/L hexaferrite particles.

Fig. 2 shows the influences of adding different amounts of anionic SDS and cationic HTAB surfactants to the electroplating bath, on the hexaferrite content and metal matrix composition of the deposited films. As can be seen from Fig. 2(a), increasing SDS concentration in the electroplating bath, from 0 to 1 g/L led to a gradual increase of hexaferrite particles incorporation to the composite, but further addition of the surfactant had a negative effect. So the optimum amount of SDS in the bath seemed to be 1 g/L. Similar trend was also observed when HTAB surfactant was used, except that the optimum surfactant concentration was 0.5 g/L. On the whole, HTAB appeared to be more effective than SDS and the maximum amount of barium hexaferrite in the composite layers which was 12 wt% achieved by addition of 0.5 g/L HTAB to the electrolyte.

Since barium hexaferrite ceramic particles are not electrically conductive, normally there

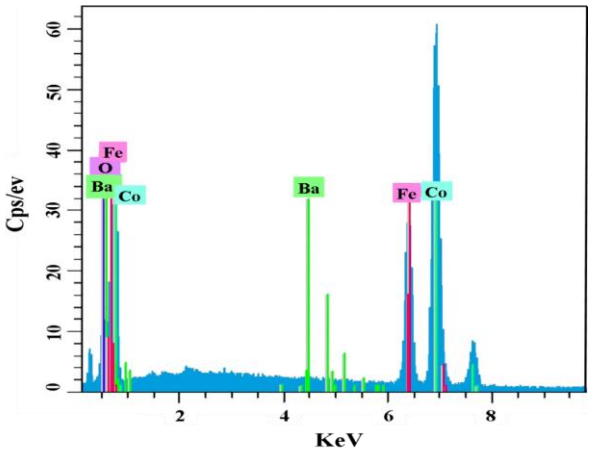

Fig. 1. EDS spectrum by analyzing the surface of the composite film obtained from a surfactant-free bath with barium hexaferrite charge of 20 g/L.

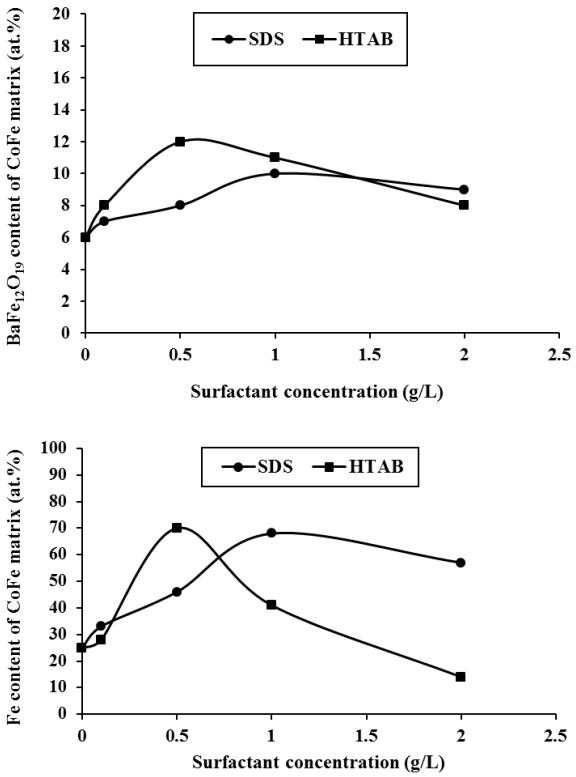

Fig. 2. Effects of surfactants and their amounts on the (a) barium hexaferrite content and (b) CoFe matrix composition of the films deposited from a bath containing 20 g/L hexaferrite nanoparticles.

is not an electrostatic attraction or repulsion between the particles and the electrode. However, due to stirring the bath, there are always some particles near the cathode surface. During electrodeposition, metal ions are reduced on the cathode and particles close to the cathode are entrapped in the growing metal film. Successful codeposition of particles occurs when the adhesion forces at cathode surface overcome the removal forces. Presence of surfactants in the electroplating bath leads to effective dispersion of particles which is helpful to their incorporation in the growing film [12]. This can generally explain the increase of hexaferrite amount with addition of surfactants. On the other hand, in solutions containing SDS, the anionic functional groups may be adsorbed on the surface of the particles and these particles are likely to be kept away from cathode. Conversely, the HTAB surfactant can charge the surface of nanoparticles with cations and make the particles suitable to be attracted by cathode. This can be the reason for higher

percentage of hexaferrite attainable in presence of the cationic surfactant.

Decreasing trend of particles codeposition when the amount of surfactants exceeds the optimum value in the plating bath is probably due to the decrease in the rate of surfactant desorption from the surface of particles in the vicinity of the cathode. At higher concentration of surfactants, the desorbed surfactant is soon substituted from the bulk of the electrolyte. Hence, the surfactant layers adsorbed on particles in the vicinity of the cathode hinder approaching of other particles to the cathode because of the repulsive interaction between ionic groups [24].

According to Fig. 2(b), a gradual rise in the iron content of the CoFe alloy matrix is noticed by increasing the amount of SDS from 0 to 1 g/L. Further increase of SDS, slightly reduced the amount of iron in the coating. As can be inferred from the diagram, changes in atomic percentage of Fe were greater when the cationic HTAB surfactant was used. Maximum amount of iron content happened in 0.5 g/L HTAB and finally 2 g/L of the surfactant resulted in a Co-rich matrix in which the Fe content was even lower than the films deposited from surfactant-free solutions. It seems the anomalous CoFe deposition is favored in presence of the barium hexaferrite nanoparticles, which can be attributed to the potential extension in cathodic direction due to surface coverage by particles.

Fig. 3 compares XRD patterns for the films deposited from a surfactant free bath containing 20 g/L hexaferrite particles with those obtained in presence of optimum values of the surfactants. Because of the small thickness (about 2µm) of the deposited films, the spectrum peaks belonged to the brass substrate showed high intensity. It can be seen that codeposition of binary alloy and barium hexaferrite particles well occurred. The deposits showed a two-phase BCC+FCC structure in all cases. The peak related to the BCC phase was sharper when deposition took place in presence of the optimum concentrations of the surfactants. Moreover, comparing the diffraction diagrams in Fig. 3 reveals that addition of surfactants intensified

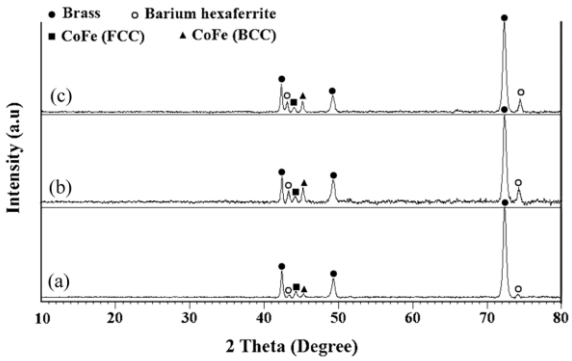

Fig. 3. X-ray diffraction patterns for the composite films deposited from a bath containing 20 g/L barium hexaferrite nanoparticles, (a) without surfactant, (b) with 1 g/L SDS surfactant, (c) with 0.5 g/L HTAB surfactant.

the peaks related to barium hexaferrite phase which means that surfactants persuaded incorporation of the particles to the CoFe matrix. This is in a good agreement with EDS results (Fig. 2(a)).

Fig. 4 shows the surface morphology of the thin films obtained from a bath containing 20 g/L hexaferrite, in absence or presence of surfactants. As shown in the figure, CoFe alloy enveloped the hexaferrite particles in all cases. Fig. 4(a) implies that without a surfactant in the deposition bath, nanoparticles have not dispersed well in the solution which consequently has caused agglomeration and non-homogenous distribution of particles in deposits. Fig. 4(d) shows a higher magnification micrograph of the agglomerative nanoparticles with polyhedral plate-like shape. In presence of anionic SDS surfactant, deposited films exhibited more uniform dissemination of the particles with minor agglomerations (Fig. 4(b) and (e)). These samples had a homogenous nodular morphology like the surfactant-free films with some micro-voids on their surfaces. A tentative explanation is that the hydrogen evolution on the cathode typically affects crystallization via absorption of the active molecule at a number of growth sites on the surface of pre-critical nuclei. This situation slows down nucleation and persuades growth, which results in a nodular morphology. Moreover, the dominant hydrogen evolution enhances formation of the pores, because the reduced hydrogen can diffuse into the deposit

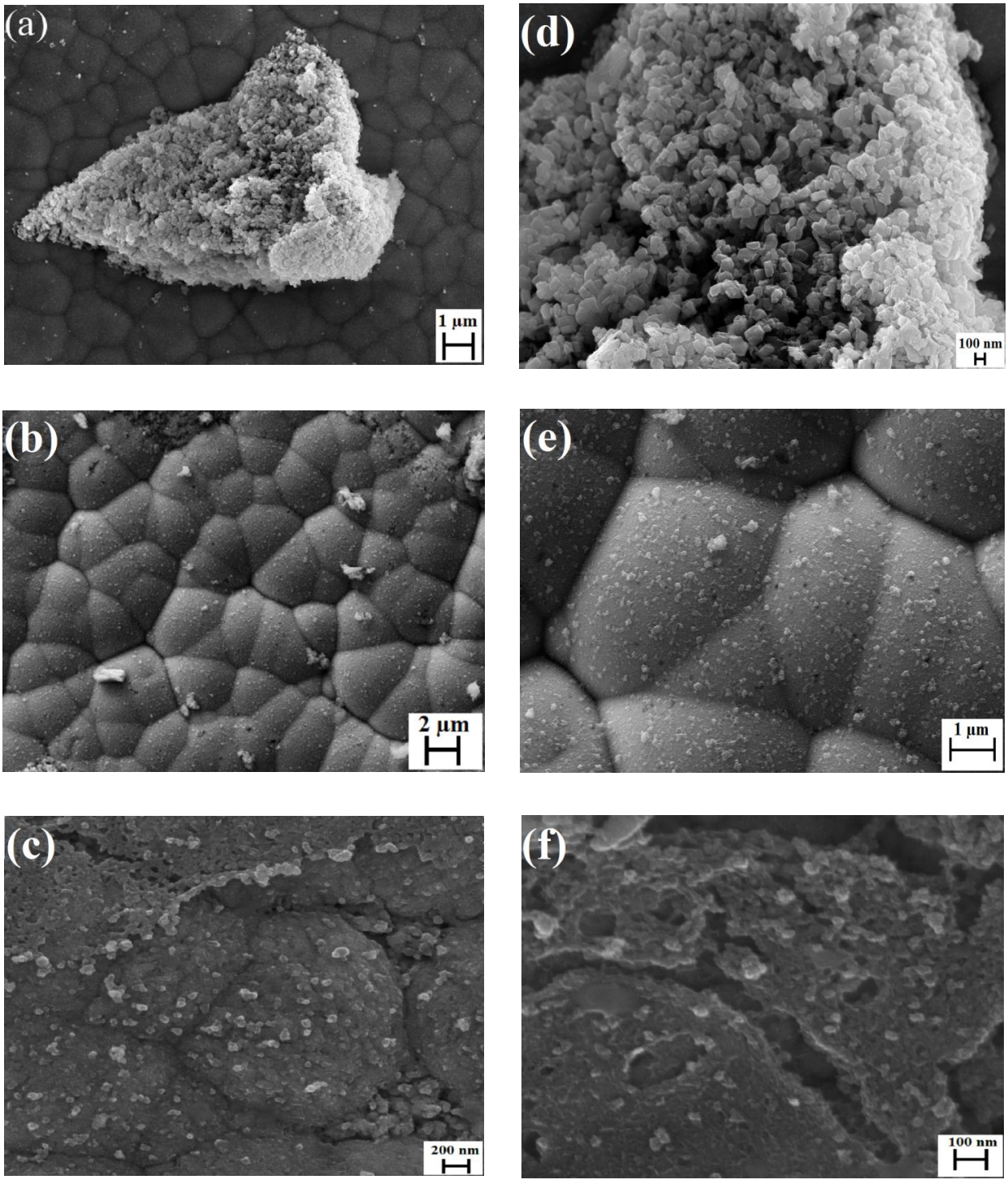

Fig. 4. FE-SEM images of the thin films deposited from a bath having 20 g/L barium hexaferrite and containing (a) no surfactant, (b) 1 g/L SDS, (c) 1g/L HTAB, (d-f) higher magnifications for (a-c)..

during the plating process [15]. Nevertheless, codeposited layers of the HTAB system presented a rough and coarse morphology with lower homogeneity (Fig. 4(c)). Furthermore, acicular growths were observable in magnified micrograph (Fig. 4(f)) unlike the relatively smooth morphologies noticed in the former deposits. Besides, addition of HTAB to the solution resulted in poor adhesion between the substrate and the deposited film, which was evident from the visual observation of the samples. It could be due to the large amount of

hydrogen diffused in the deposits which is responsible for the internal stress by causing a temporary lattice expansion in the deposited alloy [15].

4. Conclusions

CoFe-barium hexaferrite nanocomposite thin films were electrodeposited via a pulse method from an optimized bath containing 20 g/L hexaferrite nanoparticles. Effects of various concentrations of anionic SDS and cationic HTAB surfactants on the deposited films were studied and following points were concluded:

1. Increasing the concentrations of both surfactants in the electrolyte enhanced particles percentage in the deposit up to a certain amount of the surfactants, beyond which a decreasing trend of incorporated particles was observed.
2. The highest incorporation of hexaferrite particles was 12 wt% that was achieved by adding 0.5 g/L of HTAB to the electrolyte.
3. Iron content of the deposit's matrix was initially increased by increasing the surfactant amounts and experienced a drop afterwards.
4. The morphologies of the films deposited from solutions containing HTAB were coarser than the deposits achieved from electrolytes containing SDS surfactant.

Acknowledgements

The financial supports of this work by the University of Tehran and Iran Nanotechnology Initiative Council are gratefully acknowledged.

References

1. Lee, H., Cho, C., *J. Mater. Process. Technol.* Vol. 201 (2008) pp. 678–682.
2. Myung, N. V., Park, D. Y., Schwartz, M., Nobe, K., Yang, H., Yang, C. –K., Judy, J. W., *Sixth Int. Symp. Magn. Mater. Process. Devices*, Proc. Electrochem. Soc. (2000) pp. 2000–29.
3. Myung, N. V., Park, D.-Y., Yoo, B.-Y., Sumodjo, P. T.A., *J. Magn. Mater.* Vol. 265 (2003) pp. 189–198.
4. Gómez, E., Pané, S., Vallés, E., *Electrochem. commun.* Vol. 7 (2005) pp.1225–1231.
5. Niarchos, D., *Sensors Actuators A Phys.* Vol. 106, (2003) pp. 255–262.
6. Pané, S., Gómez, E., Vallés, E., *Electrochem. commun.* Vol. 9, (2007) pp. 1755–1760.
7. Cojocaru, P., Magagnin, L., Gomez, E., Vallés, E., *Mater. Lett.* Vol. 65, (2011) pp. 2765–2768.
8. Pané, S., Gómez, E., García-Amorós, J., Velasco, D., Vallés, E., *J. Electroanal. Chem.* Vol. 604, (2007) pp. 41–47.
9. Elbuken, C., Yavuz, M., Khamesee, M. B., *J., Appl. Phys.* Vol. 104, (2008) pp. 044905(1-6).
10. Yoo, B. Y., Hernandez, S. C., Park, D. –Y., Myung, N. V., *Electrochim. Acta* Vol. 51, (2006) 6346–6352.
11. Guan, S., Nelson, B. J., *J. Magn. Magn. Mater.* Vol. 292, (2005) pp. 49–58.
12. Guo, C., Zuo, Y., Zhao, X., Zhao, J., Xiong, J., *Surf. Coatings Technol.* Vol. 202, (2008) pp. 3385–3390.
13. Gómez, E., Pané, S., Alcobe, X., Vallés, E., *Electrochim. Acta* Vol. 51, (2006) pp. 5703–5709.
14. Ger, M.-D., Hou, K.-H., Hwang, B.-J., *Mater. Chem. Phys.* Vol. 87, (2004) pp. 102–108.
15. Liao, L., Liu, W., Xiao, X., J. *Electroanal. Chem.* Vol. 566, (2004) pp. 341–350.
16. Crozier, B., Liu, Q., Ivey, D. G., *J Mater Sci: Mater Electron* Vol. 22 (2011) pp. 614–625..
17. Luborsky, E. E., Livingston, J. D., Chin, G. Y.,(R. W. Cahn,& P. Haasen (eds.), *Magnetic properties of metals and alloys* (1996) pp. 2502-2565, Elsevier Science BV).
18. Osaka, T., Sayama, J.,*Electrochim. Acta*Vol. 52,(2007) pp. 2884–2890.
19. Mehrizi, S., Sohi, M. H., Shafahian, E., Khangholi, A. A., *J. Mater. Sci.: Mater. Electron*Vol. 23,(2012) pp. 1174–1181.
20. Ohnuma, S., Fujimori, H., Masumoto, T., *Appl. Phys. Lett.*Vol. 82,No. 6, (2003) pp. 946-948.
21. Montazeri-Pour, M., Ataie, A.,*J. Mater. Sci. Technol.* Vol.25, No.4,(2009) pp. 465–469.
22. Ataie, A., Montazeri-Pour, M., *Int. J. Nanosci.*Vol. 10, Nos. 4 & 5, (2011) pp. 1083-1086.
23. Khameneh, S. K., Sohi, M. H., Ataie, A., Mehrizi, S., *Adv. Mater. Res.* Vol. 829, (2013) pp. 332–336.
24. Shrestha, N. K., Masuko, M., Saji, T., *Wear* Vol. 254, (2003) pp. 555–564.